Neuron, Vol. 40, 847–858, November 13, 2003, Copyright ©2003 by Cell Press

Functional and Structural Alterations of the Intraparietal Sulcus in a Developmental Dyscalculia of Genetic Origin

Nicolas Molko,[1,*] Arnaud Cachia,[2,3] Denis Rivière,[1,2] Jean-François Mangin,[2] Marie Bruandet,[1] Denis Le Bihan,[2] Laurent Cohen,[1,4] and Stanislas Dehaene[1]
[1]INSERM U 562
Cognitive Neuroimaging
[2]Unité de Neuro-Activation Fonctionnelle and
[3]INSERM ERM 0205
Service Hospitalier Frédéric Joliot
CEA/DSV, IFR 49
Orsay
[4]Service de Neurologie 1, IFR 49
Hôpital Pitié-Salpétrière
Paris
France

Summary

Cognitive theories of numerical representation suggest that understanding of numerical quantities is driven by a magnitude representation associated with the intraparietal sulcus and possibly under genetic control. The aim of this study was to investigate, using fMRI and structural imaging, the interaction between the abnormal development of numerical representation in an X-linked condition, Turner syndrome (TS), and the development of the intraparietal sulcus. fMRI during exact and approximate calculation in TS showed an abnormal modulation of intraparietal activations as a function of number size. Morphological analysis revealed an abnormal length, depth, and sulcal geometry of the right intraparietal sulcus, suggesting an important disorganization of this region in TS. Thus, a genetic form of developmental dyscalculia can be related to both functional and structural anomalies of the right intraparietal sulcus, suggesting a crucial role of this region in the development of arithmetic abilities.

Introduction

Developmental dyscalculia is defined as an unexpected difficulty in learning arithmetic that cannot be explained by mental retardation, inappropriate schooling, or poor social environment (Kosc, 1974). While many studies have investigated the neuropsychological profiles and the cerebral bases of dyslexia (Klingberg et al., 2000; Paulesu et al., 2001; Shaywitz et al., 1995), little is known concerning the cerebral bases of developmental dyscalculia. Neuroimaging studies in developmental dyscalculia are impeded by the heterogeneity of arithmetic difficulties and by the frequent association with dyslexia and/or attention disorders. Indeed, a great variety of nonspecific problems, including slow speed of processing, poor working memory span, attentional disorders, and deficits in the long-term retrieval of arithmetic facts, may influence arithmetic performance (Temple and Sherwood, 2002). The study of genetic conditions allows us to go beyond these limitations by studying a homogeneous neurobiological phenotype. Here, we show that the study of a genetic type of developmental dyscalculia, associated with Turner syndrome, can reveal functional and structural differences in the intraparietal sulcus, a region thought to be critical for numerical representation.

Current cognitive theories assume that a supramodal abstract representation of numbers conveys the semantic information of numbers (Dehaene and Cohen, 1995). Neuropsychological studies of patients with left parietal lesions support the existence of a distinct semantic system for numerical quantities, showing that numbers double dissociate from other categories of words at the semantic level (Cappelletti et al., 1991, 2001; Dehaene and Cohen, 1997). In normal subjects, converging neuroimaging results demonstrate that active manipulation of numbers, for instance during calculation or number comparison tasks, systematically activates the horizontal segment of intraparietal sulci independently of the notation used for the numbers (Chochon et al., 1999; Dehaene et al., 1999; Gruber et al., 2001; Naccache et al., 2002; Pesenti et al., 2000; Pinel et al., 2001). Even the simple presentation of numbers without explicit magnitude processing appears sufficient to specifically activate the intraparietal sulci (Eger et al., 2003). Together, these results suggest that number-driven intraparietal activations reflect automatic access to an abstract representation of numerical quantity.

Some genetic disorders such as Turner syndrome, Williams syndrome, or Fragile X syndrome are known to lead to developmental dyscalculia (Reiss et al., 2000). In particular, subjects with Turner syndrome (TS), a genetic condition resulting from a partial or complete absence of one of the two X chromosome in a phenotypic female, typically experience visuo-spatial and number processing deficits in the absence of mental retardation and verbal disability (Ross et al., 2000). TS occurs in approximately 1 female in 2500 and is associated with well-documented physical disorders (including short stature, webbed neck, and low set ears) and abnormal estrogen production and pubertal development (Ranke and Saenger, 2001). While the severity of the cognitive profile in TS varies widely, some hallmark symptoms include deficits in visuo-spatial and number processing, executive function, and social cognition (Ross et al., 2000). Arithmetic difficulties in TS subjects are particularly evident on subtractions and operations with large numbers, subitizing, and cognitive estimation (Alexander and Money, 1966; Bruandet et al., 2003; Rovet et al., 1994; Temple and Marriot, 1998). The association of developmental dyscalculia and visuo-spatial-processing deficits in TS may reflect the intimate relationship between number and visuo-spatial representations (Dehaene et al., 1993; Fischer et al., 2003; Zorzi et al., 2002) and points toward a "spatial" subtype of dyscalculia, presumably related to an abnormal developmental trajectory of numerical representation.

Previous anatomical MRI studies in TS have not re-

*Correspondence: molko@wanadoo.fr

vealed any anomaly apparent on visual inspection, but volumetric MRI studies have shown a bilateral decrease in gray matter volume in the parietal lobes and in parieto-occipital regions as well as a reduced volume of bilateral subcortical and hippocampal gray matter (Brown et al., 2002; Murphy et al., 1993; Reiss et al., 1995). Functional neuro-imaging studies using positron emission tomography (PET) in TS have shown a decrease in glucose metabolism in parietal and occipital regions, and in the temporal cortex and insula (Clark et al., 1990; Murphy et al., 1997).

In the current study, we provide a more direct link between the abnormal development of the intraparietal sulcus and dyscalculia by studying 14 TS subjects using functional and structural imaging. First, we examine the arithmetic performance of subjects with TS and the functional correlates of calculation impairments using fMRI. We use a previously reported experimental design, including exact and approximate addition tasks, that examines both the impact of number size on parietal activation and its modulation depending on the emphasis that the task places on quantity processing (Dehaene et al., 1999). In controls, the comparison of these two numerical tasks, with virtually identical input and output requirements, has shown the use of distinct cognitive strategies: exact calculation with small numbers is acquired in a language-specific format and recruits networks involved in linguistic processes, whereas approximate and exact calculation with large numbers rely on nonverbal quantity manipulation and recruit bilaterally the intraparietal sulci (Dehaene et al., 1999; Stanescu-Cosson et al., 2000). We demonstrate that this functional pattern is disorganized in TS subjects. Second, using complementary morphometric measures, we investigate the anatomical bases of the anomalies found in fMRI and show an unusual pattern of gyrification in the intraparietal region which is abnormally activated during calculation tasks.

Results

Behavioral Results

We compared behavioral data from 14 Turner subjects (TS) and 14 normal controls. TS subjects performed significantly worse than controls on Warrington's graded arithmetic test. The mean percentage of correct responses, ± 1 standard error, was $41.1\% \pm 4.5\%$ for TS and $60.1\% \pm 4.2\%$ for controls, $t(26) = 2.85$, $p = 0.008$. TS subjects were also impaired on a computerized word reading test. Although both groups performed close to ceiling in reading either words or pseudo-words (>92% correct), TS subjects were slower in reading both types of stimuli [words: 841 versus 646 ms, $t(26) = 2.57$, $p = 0.016$; pseudo-words: 1092 versus 860 ms, $t(22) = 2.68$, $p = 0.013$].

We analyzed behavioral performance on the exact and approximate calculation tasks performed during fMRI scanning (Figure 1). In control subjects, there was no significant difference between exact and approximate calculation in response times (RTs) or in error rates. There was, however, a significant main effect of number size [RTs: $F(1,12) = 16.9$, $p = 0.001$; errors: $F(1,12) = 32.5$, $p < 0.0001$], with larger numbers inducing responses that were 231 ms slower and that contained 9% more errors than did smaller numbers. Finally, a size by task interaction indicated that the size effect was larger in exact calculation than in approximation [RTs: $F(1,12) = 12.4$, $p = 0.004$; errors: $F(1,12) = 5.23$, $p = 0.041$].

We then examined the differences between groups. Overall, TS subjects were slower and made more errors than the controls on the number tasks. However, those differences did not reach significance [RTs: 796 versus 682 ms, $F(1,25) = 2.40$, $p = 0.13$; errors: 12.0% versus 7.3%, $F(1,25) = 3.71$, $p = 0.065$]. The only significant effect involving the group factor was a triple interaction of size, task, and group [$F(1,25) = 4.69$, $p = 0.04$]. As shown in Figure 1, like the controls, TS subjects showed a number size effect [$F(1,13) = 22.6$, $p = 0.0004$] and a size by task interaction [$F(1,13) = 17.5$, $p = 0.001$], but they were disproportionately slower in the exact condition with large numbers [RTs: 1070 versus 811 ms, $F(1,25) = 3.28$, $p = 0.08$]. A similar trend was observed in the error rates, with up to 20.5% errors in the exact large number condition in TS subjects, though none of the differences involving error rates reached significance.

Another interesting difference emerged when we compared the number tasks with the letter-matching control task. A task by group interaction indicated that TS subjects responded more slowly than the controls in the number tasks relative to the letter task [$F(1,21) = 7.72$, $p = 0.010$], though no such difference emerged on error rates ($p = 0.13$). This suggests that number processing caused greater difficulty for the patients than did the letter task.

In summary, the behavioral results confirmed that the patients were impaired in number processing, on both a standardized arithmetic battery and the specific cognitive tests that we used during fMRI. The numerical impairment was mild, affecting mostly response times to exact calculation with large numbers, and was significantly greater than on a corresponding letter processing task. Importantly, Turner subjects performed the requested fMRI tasks accurately, some of them at a normal speed, thus providing ideal conditions to compare their fMRI activation patterns with those of normal subjects.

fMRI Results

Number Processing in Controls

We first report cerebral activation in controls, and compare the results to those of a previous fMRI study using a similar paradigm (Dehaene et al., 1999).

Overall Activation

Regions activated during all the number processing tasks versus rest replicate the classical fronto-parietal network found in various studies of number processing (Table 1, Figure 2). All of these areas were also activated for the letter-matching task. While in our previous study the intraparietal sulci were more activated during calculation than during the letter-matching task, in the present study the level of activation was similar in both tasks. This suggests a tight intermingling within the parietal lobe of numerical circuits and of spatial working memory circuits needed for the letter tasks (see Grüber et al. [1999] for a similar result).

Number Size Effect

As in our previous study, number size had an impact on brain activation in exact calculation, while no impact

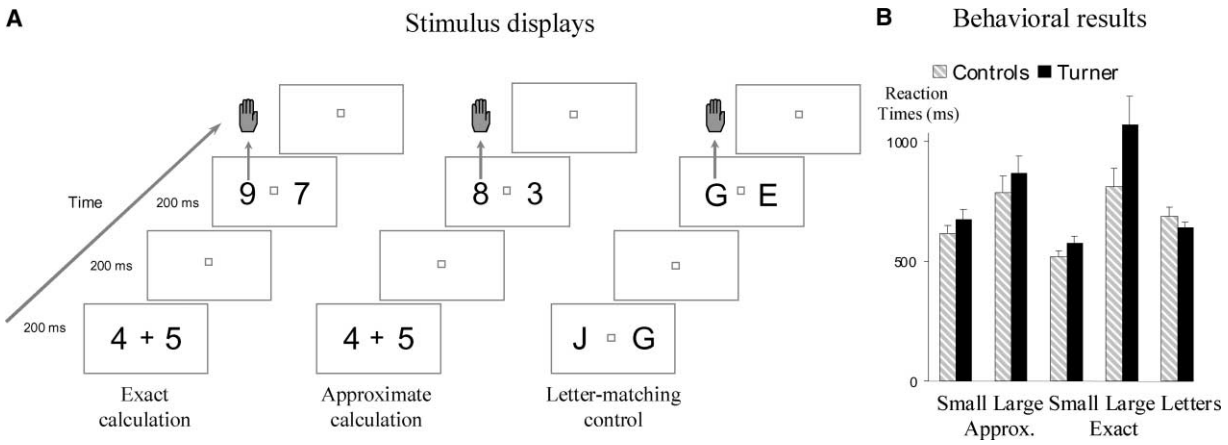

Figure 1. Behavioral Study during fMRI

(A) Examples of stimulus displays used in the three tasks during fMRI.

(B) Reaction times recorded during fMRI. The triple interaction of size, task, and group indicate that TS subjects were significantly slower than controls in exact calculation with large numbers ($p < 0.05$).

of number size was found during approximate calculation (Table 2, Figure 2). This resulted in a significant size by task interaction in three areas, the left intraparietal sulcus at TC −44, −48, 52 (125 voxels, $Z = 5.15$, $p < 0.001$), the right intraparietal sulcus at TC 44, −48, 44 (67 voxels, $Z = 4.24$, $p < 0.001$), and the right precuneus at TC 4, −60, 52 (24 voxels, $Z = 3.93$, $p = 0.01$). These three regions, which form a subset of those showing a size effect in exact calculation, may thus be considered as the cerebral basis of the behavioral number size effect.

Exact and Approximate Calculation

The distinct pattern of cerebral activation for exact and approximate calculation was also partially replicated. There was a trend toward greater activation in approximate relative to exact calculation in the right intraparietal sulcus at TC 32, −52, 56 (16 voxels, $p = 0.06$, $Z = 3.58$). This trend became significant for the left and right

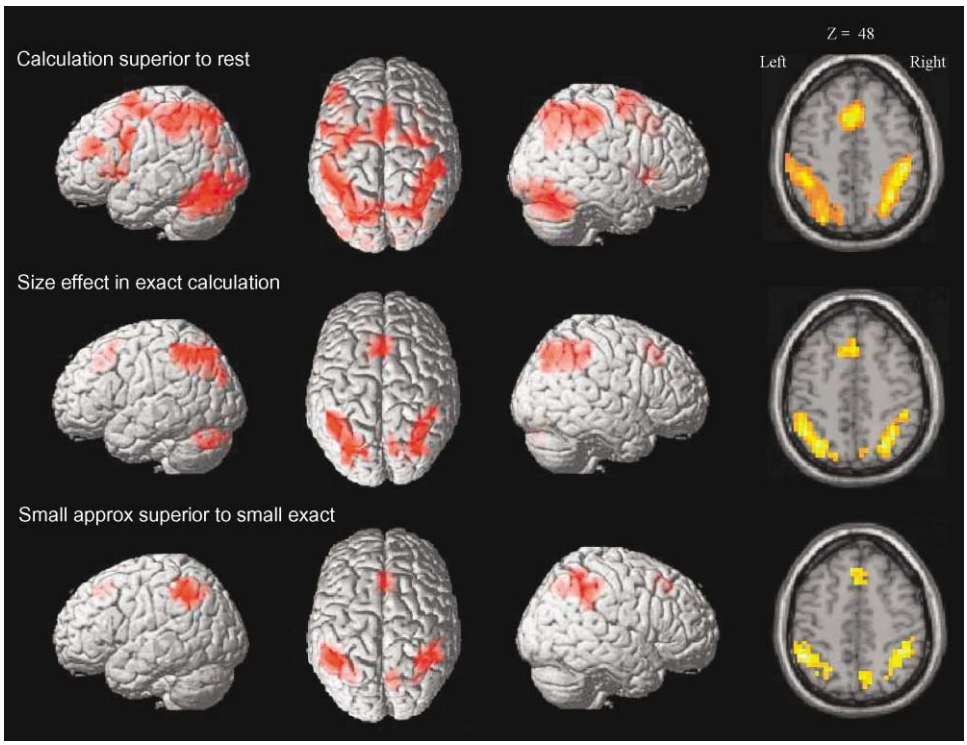

Figure 2. Brain Activation during Calculation Tasks in Controls

A bilateral fronto-parietal network, including the intraparietal sulci, was found to be activated during calculation tasks. Intraparietal activation increased with number size in exact calculation and was larger in approximate than in exact calculation, presumably related to an increase in quantity manipulation.

Table 1. Brain Regions Activated during All the Calculation Tasks Relative to Rest

Anatomical Region	Number of Voxels (1 Voxel = 64 mm^3)	Z Score Voxel Level	Talairach Coordinates x, y, z
Controls			
Bilaterial inferior occipital cortex (BA 18, 19)	1023	6.29	−44, −64, −20
Right cerebellum		6.09	24, −64, −28
Left cerebellum		5.70	−36, −48, −24
Right intraparietal sulcus (BA 7, 19, 39, 40)	1053	5.92	44, −32, 44
Left intraparietal sulcus (BA 7, 19, 39, 40)		5.87	−44, −40, 44
Left anterior cingulate cortex (BA 32)		5.72	0, 12, 52
Left middle and inferior frontal gyrus (BA 9, 44)	67	5.13	−52, 8, 28
Left dorsolateral prefrontal cortex (BA 9, 46)	45	4.84	−48, 40, 24
Left frontal operculum (BA 44)	47	4.63	−36, 28, 4
Right dorsal premotor cortex (BA 6)	50	4.04	16, 0, 72
Right caudate nucleus	30	3.87	8, 0, 8
TS subjects			
Left dorsal premotor cortex (BA 6)	250	6.06	−48, 12, 4
Left frontal operculum (BA 44)			−52, 8, 32
Right intraparietal sulcus (BA 7, 19, 39, 40)	272	6.01	28, −64, 52
Left and right anterior cingulate cortex (BA 32)	184	5.99	4, 12, 44
Left intraparietal sulcus (BA 7, 19, 39, 40)	286	5.87	−40, −44, 40
Left inferior occipital cortex (BA 18, 19), left cerebellum	264	5.44	−48, −64, −16
Right inferior occipital cortex (BA 18, 19)	260	5.44	28, −64, 32
Right frontal operculum (BA 44)	38	5.29	36, 20, 4
Left dorsolateral prefrontal cortex (BA 9, 46)	36	4.85	−32, 48, 28
Right middle and inferior frontal gyrus (BA 9, 44)	94	4.64	36, 0, 44
Right caudate nucleus	34	4.51	16, −8, 16
Left precentral cortex (BA 4)	54	4.42	−28, −8, 56
Cerebellum vermis	94	4.39	0, −64, −24
Right dorsolateral prefrontal cortex (BA 9)	38	4.25	32, 32, 44
Left lenticular nucleus	38	4.21	−24, 0, 8

intraparietal sulci when the analysis was restricted to calculations with small numbers (Table 3, Figure 2). In contrast with the previous study, no region showed greater activation during exact relative to approximate calculation. It is possible that the use of a simpler design (fixed task compared to rest), which no longer required fast switching between tasks within an fMRI run, reduced the reliance on some of the brain regions previously reported, including the rostral inferior prefrontal cortex (Koechlin et al., 1999).

Number Processing in TS Subjects

Overall Activation

During calculation relative to rest, the cerebral network activated in TS subjects overlapped considerably with the one observed in controls (Table 1). Only the anterior cingulate cortex, at TC −12, 40, 32, was significantly less activated in the TS group than in controls (110 voxels, $Z = 3.10$, $p = 0.011$). No region was significantly more activated in the TS group.

Number Size Effect

In contrast to controls, no size effect was observed during exact calculation in TS subjects, resulting in a significant interaction between group and number size in exact calculation in the right intraparietal sulcus (Table 2 and Figure 3). No interaction between number size and calculation tasks was observed in TS subjects, resulting in a significant group difference in the size by task interaction in the left intraparietal sulcus at TC −44, −48, 52 (260 voxels, $Z = 4.25$, $p < 0.001$) and in the right intraparietal sulcus at TC 44, −28, 44 (207

Table 2. Areas Showing an Effect of Number Size during Exact Calculation

Anatomical Region	Number of Voxels (1 Voxel = 64 mm^3)	Z Score Voxel Level	Talairach Coordinates x, y, z
Controls			
Left intraparietal sulcus (BA 7, 19, 39, 40)	187	5.54	−44, −52, 52
Right intraparietal sulcus (BA 7, 19, 39, 40)	157	5.17	28, −68, 48
Left and right cerebellum	30	4.51	−12, −76, −32
Left and right anterior cingulate cortex (BA 32)	70	4.29	0, 20, 48
Right middle prefrontal gyrus (BA 9)	18	4.25	24, 12, 56
Right precuneus (BA 7)	23	4.12	12, −72, 40
Left cerebellum	29	3.69	−32, −68, −36
TS subjects			
No foci of activation			
Controls superior to TS subjects			
Right intraparietal sulcus (BA 7, 39, 40)	207	4.29	48, −36, 48
TS subjects superior to Controls			
No foci of activation			

Table 3. Areas Showing Greater Activation for Small Approximate Calculation Relative to Small Exact Calculation

Anatomical Region	Number of Voxels (1 Voxel = 64 mm^3)	Z Score Voxel Level	Talairach Coordinates x, y, z
Controls			
Right intraparietal sulcus (BA 7, 39, 40)	125	5.05	48, −44, 44
Left intraparietal sulcus (BA 7, 39, 40)	115	5.01	−48, −48, 48
Left and right anterior cingulate cortex (BA 32)	32	4.27	−4, 32, 48
Right precuneus (BA 7)	27	4.25	8, −64, 44
TS subjects			
No foci of activation			
Controls superior to TS subjects			
Left caudate nucleus	333	4.34	−20, −16, 32
Right caudate nucleus		3.58	20, 4, 20
Right intraparietal sulcus (BA 7, 39, 40)		3.56	40, −40, 28
Left precuneus	463	3.90	−16, −40, 48
Left intraparietal sulcus (BA 7, 39, 40)		3.83	−48, −48, 48
TS subjects superior to Controls			
No foci of activation			

voxels, $Z = 3.62$, $p < 0.001$) (Figure 3). This result suggests a key role of the intraparietal sulci in the difficulties that TS subjects experienced in exact calculation as a function of problem size.

Exact and Approximate Calculation

No difference in the cerebral networks activated in exact and in approximate calculation was observed in TS subjects, nor between groups. However, while controls recruited the intraparietal sulci more for small approximate relative to small exact calculation, brain activation in TS subjects did not differ in this contrast. This resulted in a significant group by task interaction restricted to small numbers in the left intraparietal sulcus, left precuneus, and left caudate (Table 3, Figure 3). A nonsignificant trend toward a similar interaction was observed in the controlateral right precuneus and right posterior intraparietal region.

Morphometry

Sulcal Morphometry

We used an automatic segmentation technique to extract and measure the length and the maximal depth of

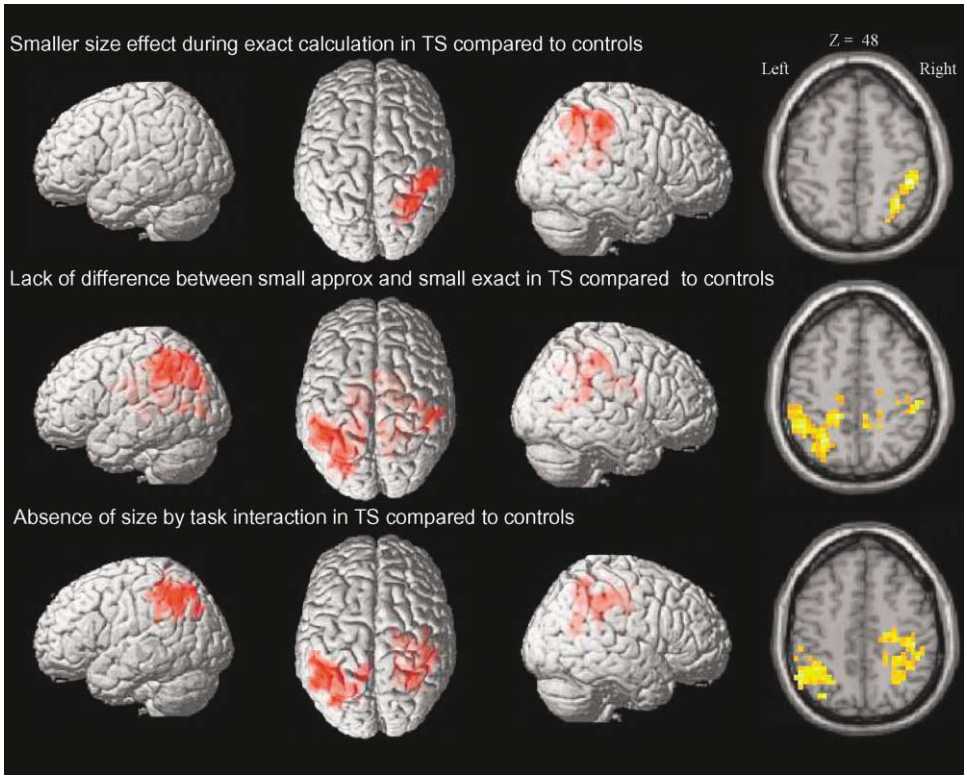

Figure 3. Brain Activation during Calculation Tasks in TS Subjects Compared to Controls

Intraparietal activation in TS subjects did not increase with number size in exact calculation, and was not larger in small approximate relative to small exact calculation. Both the left and right intraparietal sulci showed an abnormal size by task interaction in TS subjects.

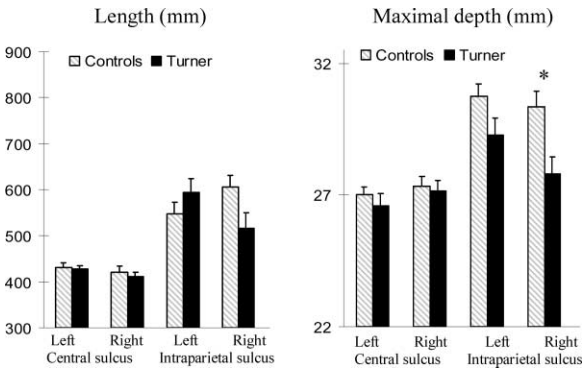

Figure 4. Histograms of Length and Maximal Depth of the Central Sulcus and the Intraparietal Sulcus

A significant decrease in maximal depth was found in the right intraparietal sulcus in TS subjects compared to controls (*p = 0.005). A nonsignificant trend toward a decrease in length of the right intraparietal sulcus was also observed.

the central sulcus and of the intraparietal sulcus. In the left and right central sulci and in the left intraparietal sulcus, no significant difference was found in these measures between the two groups (Figure 4). In contrast, a decrease in the maximal depth as well as a trend toward a reduced length ($p = 0.057$), were observed in the right intraparietal sulcus in TS subjects relative to controls (Figures 4 and 5). The center of gravity of the central sulci also showed a significant posterior displacement (along the *y* axis in Talaraich space) in TS subjects compared to controls (left central sulcus, $y = -42.6 \pm 4.4$ and $y = -30.9 \pm 4.2$, respectively, $p = 0.004$; right central sulcus, $y = -39.8 \pm 5.2$ and $y = -27.3 \pm 4.3$, respectively, $p = 0.01$) (Figure 5). Figure 5 illustrates these results, showing a roughly symmetrical sulcal pattern in controls and an asymmetrical length of the intraparietal sulcus in TS subjects.

We also investigated possible qualitative differences in the configuration of the right intraparietal sulcus. One major limitation in studies of sulcal configuration lies in the large interindividual variability of the intraparietal sulcal pattern in controls. However, although the surface appearance of the intraparietal sulcus was extremely complex and differed greatly from brain to brain, some simple features of the intraparietal sulcus were remarkably consistent across the controls (Figure 6). For instance, the antero-posterior orientation and downward convexity of the intraparietal sulcus, as well as its classical segmentation into three parts, were observed in all controls. In contrast, the right intraparietal sulcal pattern of most TS subjects did not respect these basic features because of aberrant branches, abnormal interruption, or unusual orientation (Figure 6). The three segments of the right intraparietal sulcus were observed only in 7 out of 14 TS subjects due to an absence of either the anterior or the descending part of the sulcus. The main orientation of the sulcus was highly variable in the TS group, and the downward convexity of the sulcus was observed only in three TS subjects. Finally, an unusual configuration of the horizontal segment of the right intraparietal sulcus was found in six TS subjects, due to sulcal interruption, an upward-oriented V-shape, and aberrant branches or ending (Figure 6).

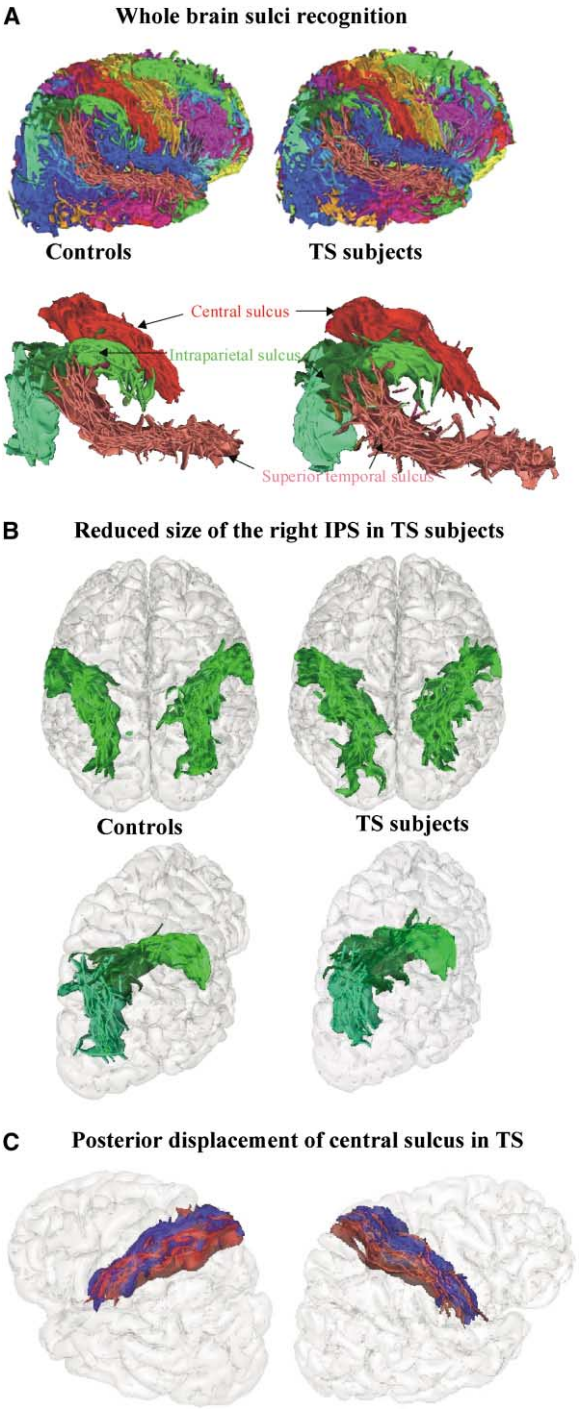

Figure 5. Comparison of TS and Rostral Subjects Using Sulcal Morphometry

(A) Superimposed images of the automatic sulci recognition algorithm in the right hemisphere of all controls and all TS subjects, with zoom on the intraparietal region.

(B) While, in controls, the left and right intraparietal sulci (IPS) appeared symmetric, the right IPS of TS had a reduced length compared to the left IPS. Compared to controls, the right IPS of TS subjects appeared both smaller and more variable, leading to a more blurry aspect of the sulcal geometry.

(C) The central sulci in TS subjects, shown in red, had a more posterior location compared to the control ones, shown in blue, presumably related to bilateral parietal atrophy.

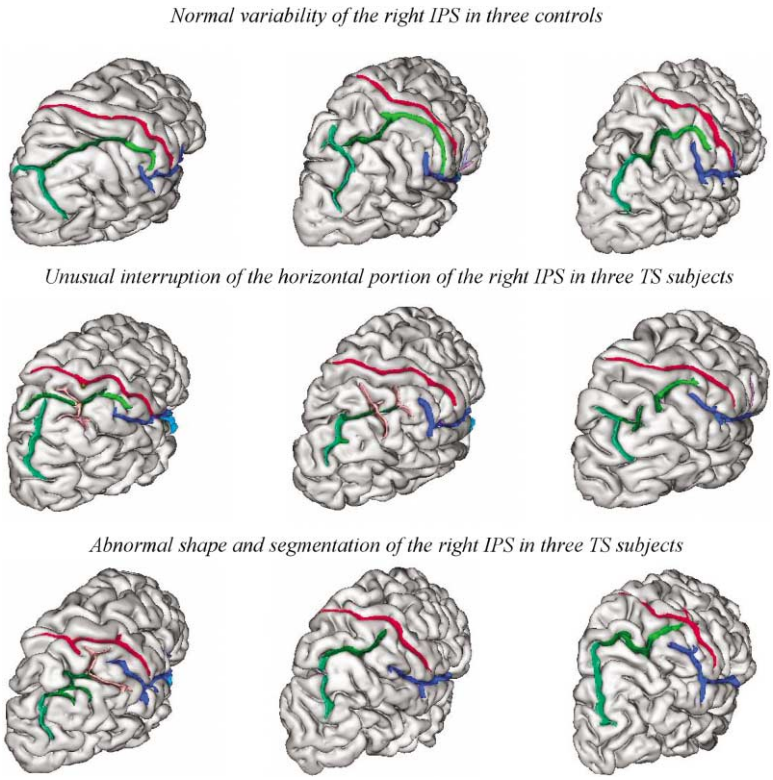

Figure 6. Anatomy of the Right Intraparietal Sulcus in Representative Control and TS Subjects

In controls (first row), despite the high variability, basic features of the intraparietal sulcus (IPS), such as its orientation with a downward concavity and its segmentation in three well-defined parts are consistently found (light green, anterior ascending segment [inferior postcentral sulcus]; dark green, horizontal segment; light blue, posterior descending segment). In many TS subjects, the shape of the sulcus appeared abnormal due to unusual interruption of the horizontal segment of the IPS, to numerous small branches (shown in pink), or to an unusual ending.

Voxel-Based Morphometry

We also analyzed our data for differences in voxel-by-voxel gray matter density. The result of this analysis is summarized in Table 4. After restriction of the analysis to the parietal lobe, only a small and marginally significant decrease in gray matter density was found in TS subjects in the depth of the right intraparietal sulcus (coordinates 43, −30, 37), close to the abnormal activation found in fMRI. Another decrease was found in the left central sulcus, while increases in gray matter were observed in the right central sulcus and left occipito-parietal sulcus. Note that the voxel-based approach is dependent on a prior whole-brain normalization, which does not take into account the localization of individual sulci. Thus, the observed differences could be spurious consequences of the displaced sulci in TS subjects.

Discussion

The main goal of this study was to investigate the functional activation and the morphology of the intraparietal sulcus, a region thought to be critical for the representation of numbers in adults, in a developmental dyscalculia of genetic origin. fMRI revealed a functional correlate of the arithmetic impairment: there was an insufficient recruitment of the right intraparietal sulcus as a function of number size. The morphological analysis showed an abnormal length, depth, and sulcal geometry of the right intraparietal sulcus, reflecting an important anatomical disorganization of this region in TS.

Arithmetic difficulties in TS were subtle and characterized by slower reaction times, particularly as the size of the numbers increased, while error rate remained at a low level. This fits well with previous behavioral results in TS (Bruandet et al., 2003; Rovet et al., 1994; Temple and Marriot, 1998) and provides ideal conditions to investigate subtle developmental impairments in arithmetic. The relative preservation of arithmetic networks was supported by fMRI results showing largely overlapping networks during calculation in TS subjects and in controls. Crucially, however, fMRI revealed an abnormal modulation of intraparietal activation as a function of number size. During exact calculation, as the size of the numbers increased, a bilateral increase in activation of

Table 4. Results of Voxel-Based Morphometry

Anatomical Region	p Value Cluster Level	Number of Voxels (1 Voxel = 1 mm^3)	Z Score Voxel Level	Talairach Coordinates x, y, z
More grey matter in controls than in TS				
Left primary motor cortex	0.039	202	4.93	50, −23, 63
Right intraparietal sulcus	0.069	170	4.02	43, −30, 37
More grey matter in TS than in controls				
Right primary motor cortex	0.024	227	4.51	50, −17, 52
Left parieto-occipital region	0.014	261	4.25	−19, −74, −37

the intraparietal sulci was observed in controls, replicating earlier work (Stanescu-Cosson et al., 2000). In TS subjects, however, the level of activation of the intraparietal sulci remained unchanged. Previous studies in controls indicate that the number size effect in exact calculation is due to a progressively greater difficulty in retrieving corresponding facts in rote memory, and therefore, to an increasing reliance on alternative strategies involving quantity manipulation, such as counting or transforming the problem to a simpler one (Lefevre, 1996). The insufficient recruitment of the intraparietal sulci in TS subjects when number size increases appears to be a direct neural correlate of the arithmetic difficulties exhibited by these subjects with large numbers, and suggests that selection and/or execution of such quantity-based strategies is deficient in TS. The insufficient recruitment of parietal areas as problem difficulty increases is consistent with a recent fMRI study with Fragile X syndrome subjects, in which they were asked to resolve arithmetic problems with two or three operands (Rivera et al., 2002). Compared to controls, subjects with Fragile X failed to show an increase in activation with arithmetic difficulty in a large set of areas including both frontal and parietal regions.

The analysis of brain activation during exact and approximate calculation with small numbers also revealed an abnormal pattern of parietal activation even for such simple operations for which performance was identical in TS subjects and in controls. In controls, there was a greater bilateral activation of the intraparietal sulci during approximation than during exact calculation. This is consistent with the hypothesis that small arithmetic facts such as 2 + 3 are often retrieved from rote memory without requiring quantity manipulations (Stanescu-Cosson et al., 2000). TS subjects, however, failed to show any difference between exact and approximate calculation, thus resulting in a significant group by task interaction. The discrepancy between superficially normal behavior and an abnormal pattern of underlying activation suggests that, contrary to controls, TS subjects did not solve small exact arithmetic facts by rote retrieval, but rather used quantity manipulation strategies similar to those used in approximate calculation.

In summary, fMRI results revealed that, although partially compensated, arithmetic difficulties in TS affected not only calculations with large numbers but also the most basic knowledge of arithmetic with numbers smaller than five. We tentatively postulate that, during exact calculation with small numbers, the lack of knowledge of arithmetic facts in TS subjects was compensated for by the use of alternative strategies mainly implicating the left intraparietal sulcus. When the task involved larger numbers, however, recruitment of the intraparietal sulci could not be increased further, thus leading to an overt behavioral impairment.

Whether or not this interpretation holds, the fMRI results clearly revealed an abnormal functional activation within the horizontal segment of the intraparietal sulcus. This region fits with the putative localization of a quantity processing system, based on previous fMRI studies of normal subjects (Dehaene et al., 2003). Converging evidence from lesion studies suggests that damage to this region can cause acalculia (Dehaene and Cohen, 1997). Two previous anatomical MRI studies in developmental dyscalculia showed a clear abnormality of the left parietal cortex (Isaacs et al., 2001; Levy et al., 1999). In particular, using voxel-based morphometry in premature children with dyscalculia, Isaacs et al. (2001) observed a decrease in the gray matter density in the left intraparietal sulcus (coordinates −39, −39, 45). Similar voxel-based morphometry analyses of our data revealed a decrease in gray matter in the right intraparietal sulcus (coordinates 43, −30, 37). This location is highly consistent with the abnormal activation observed with fMRI (TC 48, −36, 48) and is also symmetrical to the one observed in the left parietal lobe of premature children. The respective roles of the left and right parietal regions in calculation remain to be fully understood. Acalculia in adulthood is generally caused by lesions of the left inferior parietal lobe (Dehaene et al., 1998). However, subtle deficits in the abstraction of numerical relations, including the basic ability to bisect a numerical interval, have been reported following a right parietal lesion (Langdon and Warrington, 1997; Zorzi et al., 2002). Furthermore, parietal activation during calculation is always bilateral, and may predominate in the right hemisphere for basic operations such as comparison and numerosity estimation (Piazza et al., 2002; Pinel et al., 2001). The present data suggest that the right parietal lobe may play an important role in early numerical development, although we cannot exclude the possibility that subtle anomalies of the left parietal lobe might additionally be observed using more refined imaging methods.

Given the high intersubject variability of the intraparietal sulcus and its coarse intersubject registration in Talaraich space (Bookstein, 2001; Thompson et al., 2000), results of voxel-based morphometry must be interpreted with caution. In order to go beyond these limitations, a specific analysis of sulcal morphology was performed using novel software for the automatic extraction and recognition of sulci (Rivière et al., 2002). While the gray-matter density differences found using voxel-based morphometry were mild and statistically weak, the new analysis showed important quantitative differences in the morphology of the intraparietal sulcus in TS subjects, whose depth and length were reduced. Importantly, the left and right central sulci as well as the left intraparietal sulcus appeared normal in this analysis, indicating that the anomalies were particularly prominent in the right intraparietal region. In addition, the central sulcus was posteriorly displaced, suggesting an atrophy of the parietal lobes as observed in previous studies. In spite of considerable variability in the intraparietal sulcal pattern in controls, some basic and consistent features of the normal intraparietal sulcus, such as its orientation and segmentation in three parts, were not respected in most of our TS subjects. We observed the presence of many additional branches, often interrupting the main course of the intraparietal sulcus. This disorganization did not seem to follow a reproducible pattern but was highly variable from subject to subject.

To explain the stable placement and orientation of the primary sulci in normal ontogeny and phylogeny, several authors assume that the basic features of gyrogenesis are under tight genetic control (Armstrong et al., 1995; Rakic, 1988). Indeed, the intraparietal sulcus figures among the deep sulci that are present in primates and that appear early during human gestation, around the

29th week (Armstrong et al., 1995; Chi et al., 1977). Finer and more superficial details, such as tertiary sulci, appear later on in development, mostly after birth, under a variety of cytoarchitectonic, connectivity, and presumably activity-dependent constraints (Armstrong et al., 1995; Van Essen, 1997). In this context, the presence of major anomalies in the right intraparietal sulcus of TS subjects suggests an early developmental alteration, perhaps prior to birth, thus pointing to the role of X-linked genes in brain development. The role of one X-linked gene in neuronal migration and gyrogenesis is clearly established since mutations in the doublecortine (DCX) (Xq22.3, q23) gene lead to a simplified gyral pattern and cortical disorganization due to abnormal neuronal migration (Olson and Walsh, 2002). Other neurobiological mechanisms might also be involved, including abnormal mechanical constraints exerted by inappropriately targeted or missing neural connections (Fryer et al., 2003). Experimental lesion studies in monkeys indicate that the disruption of afferent pathways, when occurring very early in pregnancy, can lead to the emergence of abnormal sulcal/gyral patterns (Dehay et al., 1996; Rakic, 1988). In particular, early enucleation in monkeys leads to the presence of highly variable supplementary sulci in the occipital lobe and to a reduced size of the cortical area 17, which remains, however, well differentiated and of normal thickness (Rakic, 1988). A similar early deafferentation may explain the heavily disrupted and highly variable organization of sulci in the right parietal lobe of TS subjects.

An important issue for further investigation is the extent to which the disorganization in Turner syndrome is specific to arithmetic, or reflects a more general disruption of spatial, attentional, and/or working memory networks. It could be argued that TS subjects were impaired in tasks that were also more difficult for the control subjects, particularly the exact task with large numbers, and that this could be explained by a general reduction in working memory or attention ability. Indeed, the lack of a difference in activation between the number and letter tasks fails to provide evidence that the parietal regions under study are specific to quantity processing. This might reflect a lack of sensitivity, as significant differences between number processing and other control tasks were observed by others (e.g., Eger et al., 2003; Simon et al., 2002). Furthermore, some aspects of the results of TS subjects, such as their abnormal parietal activation even in small exact calculations, or their slowness in number tasks but not in the control letter task, are not easily explained by such an interpretation. Nevertheless, we emphasize that caution is needed when inferring the cause of dyscalculia in Turner syndrome.

In summary, the observation that X-linked developmental dyscalculia can alter the basic anatomical and functional organization of the intraparietal region strengthens the hypothesis that the development of this region is laid down under genetic control in the course of both phylogenetic evolution and child development (Dehaene et al., 1998; Simon et al., 2002). Its disruption in Turner syndrome may explain the visuo-spatial and arithmetic impairments that are commonly observed in this condition. The correlation of genetic anomalies with functional and anatomical brain abnormalities provides a powerful method to narrow down the search for genes involved in cognition and in cognitive development (Barnea-Goraly et al., 2003; Eliez et al., 2001; Watkins et al., 2002). Further research with a greater number of TS subjects, including patients with partial X deletions, should characterize the variability of the intraparietal sulcal pattern in TS subjects and the direct or indirect role of X-linked genes in the development of the intraparietal cortex and of arithmetic abilities.

Experimental Procedures

Subjects

14 subjects with TS (mean age: 24.5 $\pm$ 6.0 years) were recruited from the national TS association (AGAT association) and the endocrinology department of Saint-Vincent-de Paul hospital in Paris. All had the main physical features of the TS phenotype, ten were of the 45,X karyotype, four showed a mosaic pattern (45,X/46,XX for three subjects, 45,X/46,Xi(Xq) for one subject). All but one TS subject were taking sex steroids (estrogen and progesterone). All TS subjects included in this study were either students or employed, and lived an independent life without any social help. All but one completed their high school education. The same imaging protocol was also run on 14 control subjects matched on age, sex, and laterality (mean age: 24.3 $\pm$ 3.4 years). The mean duration after high school differed significantly between TS subjects and controls (1.5 $\pm$ 0.3 and 4.4 $\pm$ 0.75 years respectively, $p = 0.002$). All subjects gave informed consent to participate in the study, which was approved by the regional ethical committee.

Arithmetic achievement was assessed using Warrington's graded arithmetic test, which is a test of arithmetic computations of increasing difficulty (Jackson and Warrington, 1986). With a time limit of 10 s per calculation, 12 additions and then 12 subtractions were orally presented ranging in difficulty from simple items made up of single digit numbers to three digit numbers. A timed reading test of ten words and ten pseudo-words was also included to provide a measure of the reading level.

Magnetic Resonance Imaging Protocol

All scans were acquired using a 1.5T Signa horizon Echospeed MRI system (General Electric Medical Systems, Milwaukee, WI). High-resolution anatomical images were acquired in the axial plane using a spoiled gradient echo sequence (124 slices 1.2 mm thick, TR = 10.3 ms, TE = 2.1 ms, TI = 600 ms) and 24 $\times$ 24 cm field of view (resolution of 0.937 $\times$ 0.937 $\times$ 1.2 mm). During each block of the fMRI protocol, 124 functional volumes sensitive to blood oxygen level dependent contrast were acquired with a T2*-weighted gradient echo, echo planar imaging sequence (TR = 4000 ms, TE = 60 ms, and 24 $\times$ 24 cm field of view [resolution of 3.75 $\times$ 3.75 $\times$ 6 mm; 19 slices]).

Functional Imaging

Procedure

Cerebral activation was studied during three experimental tasks: exact calculation, approximate calculation, and a letter-matching control task. Each experimental task was presented in random order in a block of 30 trials. Within each number task block, three sequences were shown, each comprising five small problems (involving numbers from 1 to 5) followed by a rest period, and five large problems (involving numbers from 5 to 9), followed by a second rest period. The subjects received task instructions before each block and were trained just before the MRI with the same stimuli. Subjects were not warned, however, of the alternation of small and large numbers.

Experimental Tasks

Subjects held a button in each hand and continuously fixated on a small square. During both number tasks, an addition problem was flashed for 200 ms, with the plus sign centered, followed by a 200 ms fixation interval, and then by two numerical choices, also presented for 200 ms. For the exact calculation task, they had to select

the correct sum of the addition by pressing the corresponding button as quickly as possible. For the approximate calculation task, they had to select the most plausible number between two false results. Subjects were told that, because one of the two choices was grossly false, they did not have to compute the exact addition but could rely on a coarse estimation. During the control letter-matching task, individual letters were flashed instead of numbers and subjects were asked to press the button on the side of the repeated letter. The choice of stimuli was as described by Stanescu-Cosson et al. (2000), avoiding tie problems such as 2 + 2. Stimuli were presented using a video projector and a translucent screen. The experiment was programmed using expe5 software (Pallier et al., 1997).

Image Processing and Statistical Analysis

All fMRI analyses were performed using Statistical Parameter Mapping software, version 99 (SPM99). The first four images of each block were excluded. Images were corrected for different slice acquisition times and for motion, normalized to the reference template of the Montreal Neurological Institute (MNI) using the linear transform calculated on the anatomical images, and smoothed (FWHM 5 mm). The normalized functional images had voxels of $4 \times 4 \times 4$ mm^3. The data from each subject was first analyzed using the general linear model and the theory of Gaussian random fields as implemented in SPM99 with predictors based on the known experimental blocks convolved by the standard hemodynamic function and its derivative. Group analyses were then performed with a random effect analysis of variance. We tested each calculation task versus rest and versus the letter task for brain areas showing a significant activation. The voxelwise threshold for within- and between-group comparisons was set to $p < 0.001$ and $p < 0.01$ respectively. Clusters were reported if their extent was significant at $p < 0.05$, corrected for multiple comparisons across the whole brain.

Structural Imaging

Sulcal Morphometry

The coarse intersubject registration of the intraparietal sulcus in Talaraich space imposes major limitations on voxel-based methods. We therefore also analyzed the geometry of the intraparietal and central sulci using an automatic sulcus identification procedure as described by Rivière et al. (2002). Individual sulci were extracted from high-resolution anatomical images using a procedure that converts the anatomical images to abstract representations of the cortical folding pattern. An automatic recognition algorithm, using a congregation of neural networks taught on a manually labeled database, was then applied to the main sulci of the cerebral cortex (Mangin et al., 1995; Rivière et al., 2002). As previously reported, a mean recognition rate of 76% is obtained using this method (Mangin et al., 1995; Rivière et al., 2002). Errors are mainly due to ambiguous sulcal configurations. For the studied sulci, the automatic recognition was visually verified and, if necessary, corrected. We compared the length and the maximal depth of the intraparietal sulcus and of the central sulcus between TS subjects and controls using Student's t test. The influence of putative parietal atrophy on the location of the central sulcus was tested by comparing the location of the center of gravity of the central sulcus in the two groups using Student's t test.

Voxel-Based Morphometry

To characterize the local differences in the parietal gray matter density between TS subjects and controls, we used voxel-based morphometry (VBM) (Ashburner and Friston, 2000; Good et al., 2001), investigating each hemisphere separately (Riviere et al., 2002), and used a mask to restrict the analysis to the parietal lobes. The separate analysis of each hemisphere offers two advantages. First, the normalization can be optimized with a customized template, and second, it provides a precise analysis of medial structures without the partial volume effect of the controlateral homologous region after image smoothing. As proposed in the optimized method, anatomical images were processed in three different steps: tissue segmentation, spatial normalization, and smoothing (Ashburner and Friston, 2000; Good et al., 2001). We compared the smoothed gray-matter images between TS and controls on a voxel-by-voxel basis using a one-way ANOVA. We used a voxelwise significance threshold of $p < 0.01$, and a cluster extent threshold of $p < 0.05$ corrected for multiple comparisons across the parietal volume.

Acknowledgments

We are indebted to the members of the French Turner syndrome association (AGAT) for their continued cooperation. We also wish to thank Professor Jean-Claude Carel for his help in the recruitment, and Narly Golestany for revision of the manuscript. Supported by INSERM, CEA, and a Centennial Fellowship of the Mc Donnell Foundation to S.D.

Received: July 22, 2003
Revised: September 16, 2003
Accepted: September 30, 2003
Published: November 12, 2003

References

Alexander, D., and Money, J. (1966). Turner syndrome and Gerstmannn's syndrome: neuropsychological comparison. Neuropsychologia *4*, 265–273.

Armstrong, E., Schleicher, A., Omran, H., Curtis, M., and Zilles, K. (1995). The ontogeny of human gyrification. Cereb. Cortex *5*, 56–63.

Ashburner, J., and Friston, K.J. (2000). Voxel-based morphometry—the methods. Neuroimage *11*, 805–821.

Barnea-Goraly, N., Eliez, S., Hedeus, M., Menon, V., White, C.D., Moseley, M., and Reiss, A.L. (2003). White matter tract alterations in fragile X syndrome: preliminary evidence from diffusion tensor imaging. Am. J. Med. Genet. *118B*, 81–88.

Bookstein, F.L. (2001). Voxel-based morphometry should not be used with imperfectly registered images. Neuroimage *14*, 1454–1462.

Brown, W.E., Kesler, S.R., Eliez, S., Warsofsky, I.S., Haberecht, M., Patwardhan, A., Ross, J.L., Neely, E.K., Zeng, S.M., Yankowitz, J., et al. (2002). Brain development in Turner syndrome: a magnetic resonance imaging study. Psychiatry Res. *116*, 187–196.

Bruandet, M., Molko, N., Cohen, L., and Dehaene, S. (2003). A cognitive characterisation of dyscalculia in Turner syndrome. Neuropsychologia, in press.

Cappelletti, M., Butterworth, B., and Kopelman, M. (2001). Spared numerical abilities in a case of semantic dementia. Neuropsychologia *39*, 1224–1239.

Chi, J.G., Dooling, E.C., and Gilles, F.H. (1977). Gyral development of the human brain. Ann. Neurol. *1*, 86–93.

Chochon, F., Cohen, L., van de Moortele, P.F., and Dehaene, S. (1999). Differential contributions of the left and right inferior parietal lobules to number processing. J. Cogn. Neurosci. *11*, 617–630.

Cipolotti, L., Butterworth, B., and Denes, G. (1991). A specific deficit for numbers in a case of dense acalculia. Brain *114*, 2619–2637.

Clark, C., Klonoff, H., and Hayden, M. (1990). Regional cerebral glucose metabolism in Turner syndrome. Can. J. Neurol. Sci. *17*, 140–144.

Dehaene, S., and Cohen, L. (1995). Towards an anatomical and functional model of number processing. Math. Cogn. *1*, 83–120.

Dehaene, S., and Cohen, L. (1997). Cerebral pathways for calculation: double dissociation between rote verbal and quantitative knowledge of arithmetic. Cortex *33*, 219–250.

Dehaene, S., Bossini, S., and Giraux, P. (1993). The mental representation of parity and numerical magnitude. J. Exp. Psychol. Gen. *122*, 371–396.

Dehaene, S., Dehaene-Lambertz, G., and Cohen, L. (1998). Abstract representations of numbers in the animal and human brain. Trends Neurosci. *21*, 355–361.

Dehaene, S., Spelke, E., Pinel, P., Stanescu, R., and Tsivkin, S. (1999). Sources of mathematical thinking: behavioral and brain-imaging evidence. Science *284*, 970–974.

Dehaene, S., Piazza, M., Pinel, P., and Cohen, L. (2003). Three parietal circuits for number processing. Cogn. Neuropsychol., in press.

Dehay, C., Giroud, P., Berland, M., Killackey, H., and Kennedy, H. (1996). Contribution of thalamic input to the specification of cytoarhitectonic cortical fields in the primate: effects of bilateral enucleation in the fetal monkey on the boundaries, dimensions, and gyrification of striate and extrastriate cortex. J. Comp. Neurol. *367*, 70–89.

Eger, E., Sterzer, P., Russ, M.O., Giraud, A.L., and Kleinschmidt, A. (2003). A supramodal number representation in human intraparietal cortex. Neuron *37*, 719–725.

Eliez, S., Antonarakis, S.E., Morris, M.A., Dahoun, S.P., and Reiss, A.L. (2001). Parental origin of the deletion 22q11.2 and brain development in velocardiofacial syndrome: a preliminary study. Arch. Gen. Psychiatry *58*, 64–68.

Fischer, M.H., Castel, A.D., Dodd, M.D., and Pratt, J. (2003). Perceiving numbers causes spatial shifts or attention. Nat. Neurosci. *6*, 555–556.

Fryer, S.L., Kwon, H., Eliez, S., and Reiss, A.L. (2003). Corpus callosum and posterior fossa development in monozygotic females: a morphometric MRI study of Turner syndrome. Dev. Med. Child Neurol. *45*, 320–324.

Good, C.D., Johnsrude, I.S., Ashburner, J., Henson, R.N., Friston, K.J., and Frackowiak, R.S. (2001). A voxel-based morphometric study of ageing in 465 normal adult human brains. Neuroimage *14*, 21–36.

Grüber, O., Indefrey, P., Steinmetz, H., and Kleinschmidt, A. (2001). Dissociating neural correlates of cognitive components in mental calculation. Cereb. Cortex *11*, 350–359.

Isaacs, E.B., Edmonds, C.J., Lucas, A., and Gadian, D.G. (2001). Calculation difficulties in children of very low birthweight: a neural correlate. Brain *124*, 1701–1707.

Jackson, M., and Warrington, E.K. (1986). Arithmetic skills in patients with unilateral cerebral lesions. Cortex *22*, 611–620.

Klingberg, T., Hedehus, M., Temple, E., Salz, T., Gabrieli, J.D., Moseley, M.E., and Poldrack, R.A. (2000). Microstructure of temporoparietal white matter as a basis for reading ability: evidence from diffusion tensor magnetic resonance imaging. Neuron *25*, 493–500.

Koechlin, E., Basso, G., Pietrini, P., Panzer, S., and Grafman, J. (1999). The role of the anterior prefrontal cortex in human cognition. Nature *399*, 148–151.

Kosc, L. (1974). Developmental dyscalculia. J. Learn. Disabil. *7*, 46–59.

Langdon, D.W., and Warrington, E.K. (1997). The abstraction of numerical relations: a role for the right hemisphere in arithmetic? J. Int. Neuropsychol. Soc. *3*, 260–268.

Lefevre, J.-A. (1996). Selection of procedures in mental addition: reassessing the problem-size effect in adults. J. Exp. Psychol. Learn. Mem. Cogn. *22*, 216–230.

Levy, L.M., Reis, I.L., and Grafman, J. (1999). Metabolic abnormalities detected by 1H-MRS in dyscalculia and dysgraphia. Neurology *53*, 639–641.

Mangin, J.F., Frouin, V., Bloch, I., Régis, J., and López-Krahe, J. (1995). From 3D magnetic resonance images to structural representations of the cortex topography using topology preserving deformations. J. Math. Imag. Vis. *5*, 297–318.

Murphy, D.G., DeCarli, C., Daly, E., Haxby, J.V., Allen, G., White, B.J., McIntosh, A.R., Powell, C.M., Horwitz, B., Rapoport, S.I., et al. (1993). X-chromosome effects on female brain: a magnetic resonance imaging study of Turner's syndrome. Lancet *342*, 1197–1200.

Murphy, D.G., Mentis, M.J., Pietrini, P., Grady, C., Daly, E., Haxby, J.V., De La Granja, M., Allen, G., Largay, K., White, B.J., et al. (1997). A PET study of Turner's syndrome: effects of sex steroids and the X chromosome on brain. Biol. Psychiatry *41*, 285–298.

Naccache, L., Blandin, E., and Dehaene, S. (2002). Unconscious masked priming depends on temporal attention. Psychol. Sci. *13*, 416–424.

Olson, E.C., and Walsh, C.A. (2002). Smooth, rough and upside-down neocortical development. Curr. Opin. Genet. Dev. *12*, 320–327.

Pallier, C., Dupoux, E., and Jeannin, X. (1997). Expe5: an expandable programming language for on-line psychological experiments. Behav. Res. Methods Instrum. Comput. *29*, 322–327.

Paulesu, E., Demonet, J.F., Fazio, F., McCrory, E., Chanoine, V., Brunswick, N., Cappa, S.F., Cossu, G., Habib, M., Frith, C.D., et al. (2001). Dyslexia: cultural diversity and biological unity. Science *291*, 2165–2167.

Pesenti, M., Thioux, M., Seron, X., and De Volder, A. (2000). Neuroanatomical substrates of arabic number processing, numerical comparison, and simple addition: a PET study. J. Cogn. Neurosci. *12*, 461–479.

Piazza, M., Mechelli, A., Price, C., and Butterworth, B. (2002). The quantifying brain: functional neuroanatomy of numerosity estimation and counting.

Pinel, P., Dehaene, S., Riviere, D., and LeBihan, D. (2001). Modulation of parietal activation by semantic distance in a number comparison task. Neuroimage *14*, 1013–1026.

Rakic, P. (1988). Specification of cerebral cortical areas. Science *241*, 170–176.

Ranke, M.B., and Saenger, P. (2001). Turner's syndrome. Lancet *358*, 309–314.

Reiss, A.L., Mazzocco, M.M., Greenlaw, R., Freund, L.S., and Ross, J.L. (1995). Neurodevelopmental effects of X monosomy: a volumetric imaging study. Ann. Neurol. *38*, 731–738.

Reiss, A.L., Eliez, S., Schmitt, J., Patwardhan, A., and Haberecht, M. (2000). Brain imaging in neurogenetic conditions: realizing the potential of behavioral neurogenetics research. Ment. Retard. Dev. Disabil. Res. Rev. *6*, 186–197.

Rivera, S.M., Menon, V., White, C.D., Glaser, B., and Reiss, A.L. (2002). Functional brain activation during arithmetic processing in females with Fragile X syndrome is related to FMR1 protein expression. Hum. Brain Mapp. *16*, 206–218.

Rivière, D., Mangin, J.F., Papadopoulos-Orfanos, D., Martinez, J., Frouin, V., and Regis, J. (2002). Automatic recognition of cortical sulci of the human brain using a congregation of neural networks. Med. Image Anal. *6*, 77–92.

Ross, J., Zinn, A., and McCauley, E. (2000). Neurodevelopmental and psychosocial aspects of Turner syndrome. Ment. Retard. Dev. Disabil. Res. Rev. *6*, 135–141.

Rovet, J., Szekely, C., and Hockenberry, M.N. (1994). Specific arithmetic calculation deficits in children with Turner syndrome. J. Clin. Exp. Neuropsychol. *16*, 820–839.

Shaywitz, B.A., Shaywitz, S.E., Pugh, K.R., Constable, R.T., Skudlarski, P., Fulbright, R.K., Bronen, R.A., Fletcher, J.M., Shankweiler, D.P., Katz, L., et al. (1995). Sex differences in the functional organization of the brain for language. Nature *373*, 607–609.

Simon, O., Mangin, J.F., Cohen, L., Le Bihan, D., and Dehaene, S. (2002). Topographical layout of hand, eye, calculation, and language-related areas in the human parietal lobe. Neuron *33*, 475–487.

Stanescu-Cosson, R., Pinel, P., van De Moortele, P.F., Le Bihan, D., Cohen, L., and Dehaene, S. (2000). Understanding dissociations in dyscalculia: a brain imaging study of the impact of number size on the cerebral networks for exact and approximate calculation. Brain *123*, 2240–2255.

Temple, C.M., and Marriot, A.J. (1998). Arithmetical ability and disability in Turner's syndrome: a cognitive neuropsychological analysis. Dev. Neuropsychol. *14*, 47–67.

Temple, C.M., and Sherwood, S. (2002). Representation and retrieval of arithmetical facts: developmental difficulties. Q. J. Exp. Psychol. A *55*, 733–752.

Thompson, P.M., Woods, R.P., Mega, M.S., and Toga, A.W. (2000). Mathematical/computational challenges in creating deformable and probabilistic atlases of the human brain. Hum. Brain Mapp. *9*, 81–92.

Van Essen, D.C. (1997). A tension-based theory of morphogenesis and compact wiring in the central nervous system. Nature *385*, 313–318.

Watkins, K.E., Vargha-Khadem, F., Ashburner, J., Passingham, R.E., Connelly, A., Friston, K.J., Frackowiak, R.S., Mishkin, M., and Gadian, D.G. (2002). MRI analysis of an inherited speech and language disorder: structural brain abnormalities. Brain *125*, 465–478.

Zorzi, M., Priftis, K., and Umilta, C. (2002). Brain damage: neglect disrupts the mental number line. Nature *417*, 138–139.